Science of the Total Environment 618 (2018) 388–398

Contents lists available at ScienceDirect

Science of the Total Environment

journal homepage: www.elsevier.com/locate/scitotenv

Ocean acidification dampens physiological stress response to warming and contamination in a commercially-important fish (*Argyrosomus regius*)

Eduardo Sampaio [a,*,1], Ana R. Lopes [a,b,1], Sofia Francisco [a], Jose R. Paula [a], Marta Pimentel [a], Ana L. Maulvault [a,c,d], Tiago Repolho [a], Tiago F. Grilo [a], Pedro Pousão-Ferreira [c], António Marques [c,d], Rui Rosa [a]

[a] MARE - Marine Environmental Sciences Centre & Laboratório Marítimo da Guia, Faculdade de Ciências, Universidade de Lisboa, Av. Nossa Senhora do Cabo 939, 2750-374 Cascais, Portugal
[b] UCIBIO, REQUIMTE, Departamento de Química, Faculdade de Ciências e Tecnologia, Universidade Nova de Lisboa, Quinta da Torre, 2829-516 Caparica, Portugal
[c] Divisão de Aquacultura e Valorização (DivAV), Instituto Português do Mar e da Atmosfera (IPMA, I.P.), Av. Brasília, 1449-006 Lisboa, Portugal
[d] Interdisciplinary Centre of Marine and Environmental Research (CIIMAR), University of Porto, Rua das Bragas, 289, 4050-123 Porto, Portugal

HIGHLIGHTS

- Atmospheric and water conditions/contaminants influence animal physiology status.
- Scarcely studied multi-stressor effects were extricated via full-factorial design.
- Warming stimulated mercury accumulation, but was offset by acidification.
- Co-occurring acidification countered oxidative stress elicited by other stressors.
- Enhanced mitigation pathways or chemical dynamics may underpin stressor antagonism.

GRAPHICAL ABSTRACT

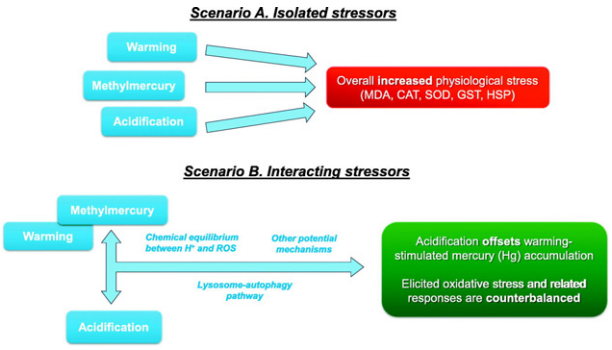

ARTICLE INFO

Article history:
Received 23 August 2017
Received in revised form 5 November 2017
Accepted 6 November 2017
Available online 11 November 2017

Editor: D. Barcelo

Keywords:
Ocean acidification
Methylmercury
Warming
Oxidative stress
Antagonistic effects
Argyrosomus regius

ABSTRACT

Increases in carbon dioxide (CO_2) and other greenhouse gases emissions are changing ocean temperature and carbonate chemistry (warming and acidification, respectively). Moreover, the simultaneous occurrence of highly toxic and persistent contaminants, such as methylmercury, will play a key role in further shaping the ecophysiology of marine organisms. Despite recent studies reporting mostly additive interactions between contaminant and climate change effects, the consequences of multi-stressor exposure are still largely unknown. Here we disentangled how *Argyrosomus regius* physiology will be affected by future stressors, by analysing organ-dependent mercury (Hg) accumulation (gills, liver and muscle) within isolated/combined warming ($\Delta T = 4$ °C) and acidification ($\Delta pCO_2 = 1100$ μatm) scenarios, as well as direct deleterious effects and phenotypic stress response over multi-stressor contexts. After 30 days of exposure, although no mortalities were observed in any treatments, Hg concentration was enhanced under warming conditions, especially in the liver. On the other hand, elevated CO_2 decreased Hg accumulation and consistently elicited a dampening effect on warming and contamination-elicited oxidative stress (catalase, superoxide dismutase and glutathione-*S*-transferase activities) and heat shock responses. Thus, potentially unpinned on CO_2-promoted protein removal and ionic equilibrium between hydrogen and reactive oxygen species, we found that co-occurring acidification decreased heavy

* Corresponding author.
E-mail address: easampaio@fc.ul.pt (E. Sampaio).
[1] Equally contributed.

https://doi.org/10.1016/j.scitotenv.2017.11.059
0048-9697/© 2017 Elsevier B.V. All rights reserved.

metal accumulation and contributed to physiological homeostasis. Although this indicates that fish can be physiologically capable of withstanding future ocean conditions, additional experiments are needed to fully understand the biochemical repercussions of interactive stressors (additive, synergistic or antagonistic).

© 2017 Elsevier B.V. All rights reserved.

1. Introduction

Atmospheric carbon dioxide (CO_2) concentrations have been increasing since the preindustrial era (recently surpassing 400 CO_2 μatm), and are expected to reach approximately 1000 CO_2 μatm by the year 2100 (IPCC, 2014). Moreover, conjointly with other "greenhouse" gases, increased CO_2 has triggered a continuous rise in mean ocean temperatures (nowadays increased by 0.76 °C from pre-industrial values), with predictions pointing to a further 0.3–4.8 °C increase by the end of the century (IPCC, 2014). Atmospheric CO_2 dissolves in the ocean, shifting seawater carbonate chemistry equilibrium. Carbon dioxide uptake increases hydrogen ion (H^+) availability, leading to a concomitant decrease of 0.13–0.42 units in mean ocean pH by the year 2100, i.e. ocean acidification (IPCC, 2014). Due to naturally frequent variations in seawater physicochemical properties (e.g. upwelling events, significant carbon input from river basins), a more accentuated CO_2 input will occur in coastal areas, easily reaching pCO_2 values beyond 1500 μatm (Melzner et al., 2013). The combined occurrence of ocean warming and acidification imposes ecophysiological challenges to marine organisms, eliciting interactive negative effects on survival, growth and overall physiological fitness (Harvey et al., 2013; Kroeker et al., 2010; Pimentel et al., 2015).

Concurrently to ocean warming and acidification, marine biota will also deal with another major stressor: contamination. One of the most concerning and persistent metal contaminants is mercury (Hg) and its ubiquitous environmental compound, methylmercury (MeHg) (Korbas et al., 2012). Often a by-product of fossil fuel combustion and unfiltered industrial processes (e.g. chloralkaline), inorganic Hg is transported to the sediments of estuaries and coastal areas, and methylated into organic MeHg by bacteria (Dijkstra et al., 2013), augmenting Hg bioavailability, bioaccumulation and biomagnification in organisms throughout the marine food web (Campbell et al., 2005; Evers et al., 2011). In teleost fish, MeHg accumulates preferentially in soft organ tissues, producing site-specific structural and functional damage (Gonzalez et al., 2005), and comprises around 90–95% of total mercury (HgT) in the organism (Burger et al., 2003; Gray et al., 2000). Due to its high affinity for thiol groups (present in key peptides and proteins), Hg accumulation can cause deleterious effects, including physiological distress, i.e. activation of antioxidant and xenobiotic defenses (Gonzalez et al., 2005; Mieiro et al., 2010), behavioural and organ functionality impairments (Berntssen et al., 2003; Sampaio et al., 2016) and ultimately mortality (Coccini et al., 2000).

Contaminant uptake and its impacts are potentially shaped by increased temperature or CO_2 and vice-versa (Noyes et al., 2009). Specifically, interactions between temperature and heavy metal contamination influence the physiological tolerance to both stress factors (Sokolova and Lannig, 2008) while exacerbating biological responses (Dorts et al., 2014; Lapointe et al., 2011; Sappal et al., 2014). Consequently, MeHg accumulation is augmented and propagation throughout the food chain is strengthened, until metabolic thresholds are reached (Dijkstra et al., 2013). In parallel, severe acidification (pH < 7) increases metal availability (Wiener et al., 1990) and toxicity (Han et al., 2014). However, such effect may be offset by CO_2-linked decreases in mercury accumulation (Sampaio et al., 2016; Schiedek et al., 2007; Wang et al., 2017). Under environmental stress, a general deleterious biochemical pathway triggered is the formation of reactive oxygen species (ROS) in organism cells. Although there is some proof linking ROS production to hypercapnic scenarios (Pimentel et al., 2015), such is particularly true for increased temperature and mercury contamination (Berntssen et al., 2003; Portner, 2002). The presence of ROS causes ion-based protein damage and lipid peroxidation in cellular membranes, i.e. oxidative stress, from which the reactive and mutagenic compound malondialdehyde (MDA) is an end-product (Lesser, 2006). As a physiological defense response, ROS production elicits antioxidant activity in the organism. Specifically, a battery of enzymes is activated to eliminate ROS and prevent MDA build-up: superoxide dismutase (SOD), which converts superoxide (O_2^-) into hydrogen peroxide (H_2O_2); catalase (CAT) which converts H_2O_2 into water (H_2O) and oxygen (O_2); and glutathione *S*-transferase (GST), which is involved in the protection against xenobiotics and linked to antioxidant defense (Lesser, 2006; Wang et al., 2000). Moreover, tissue-specific heat shock protein (Hsp70) production is also correlated with thermal stress, i.e. high temperatures (Repolho et al., 2014; Rosa et al., 2012, 2014a) and metal contamination (Rajeshkumar and Munuswamy, 2011; Williams et al., 1996). Heat shock proteins help repair, refold and eliminate damaged or denatured proteins, as well as protect and control ROS formation (Sokolova et al., 2011). Given their wide scope, these constituents of the antioxidant enzymatic and protein chaperone machineries are widely used as biomarkers in ecotoxicology to assess fish physiological stress responses (e.g. Anacleto et al., 2014; Fonseca et al., 2011; Rosa et al., 2014b; Maulvault et al., 2016).

Despite the inevitability of marine organisms having to cope with simultaneous effects of ocean warming, acidification and persistent contamination (MeHg), no studies have focused on how the interactive effects between these three stressors will challenge fish ecophysiology. The meagre (*Argyrosomus regius*) is an oceanodromous teleost fish dispersed across the eastern Atlantic, with increasing economic value within fisheries and aquaculture activities. Due to its nearshore distribution, this species is particularly susceptible to MeHg accumulation, especially when adults migrate towards estuaries to spawn (Durrieu et al., 2005). Understanding how this commercially important species will deal with the forecasted future scenarios may provide valuable information on future stock population conditions and potential impacts on coastal food-webs. To fill these knowledge gaps, we performed a 30-day acclimation experiment under future ocean conditions, in which we investigated how interacting stressors modulate physiological impacts and elicited responses on the commercially important *A. regius*. To this end, we gauged how organ-dependent Hg accumulation (gills, liver and muscle) was modulated by warming ($\Delta T = 4$ °C) and acidification ($\Delta pCO_2 = 1100$ μatm), and measured the direct consequences of isolated and combined stressor exposure at organism (survival rates and condition index) and cellular (lipid peroxidation, i.e. MDA) levels. Moreover, in order to provide a comprehensive depiction of physiological state, the phenotypic responses of antioxidant enzymatic (SOD, CAT and GST) and molecular chaperone (Hsp70) machineries were also evaluated.

2. Material and methods

2.1. Experimental setup and incubation

Juvenile *A. regius* ($n \approx 100$) (mean ± SD; total weight: 4.26 ± 2.8 g; total length: 6.30 ± 1.2 cm) were acquired from EPPO - IPMA (Estação Piloto de Piscicultura de Olhão – Instituto Português do Mar e da Atmosfera, Portugal), where standard summer season environmental parameters were maintained (pH = 8.0 and 19 °C). In August 2014,

fish were transported via land for 3 h, in tanks containing seawater and oxygen-saturated air, to the facilities of Laboratório Marítimo da Guia (LMG, MARE, Faculdade de Ciências, Universidade de Lisboa). Upon arrival, fish were randomly placed and acclimated for two weeks in twenty-four 50 l tanks (n = 3–4 per tank) with individual recirculating aquaculture systems (RAS) equipped with glass wool (physical filtration), bio-balls (Fernando Ribeiro Lda) and protein skimmers (biological filtration, ReefSkimPro 850, TMC Iberia), as well as additional UV disinfection (Vecton 120, TMC Iberia) to maintain superior water quality. Natural seawater was pumped directly from the ocean into an 8 m^3 storage tank, and subsequently filtered (0.35 μm filters, Fernando Ribeiro Lda) and UV-sterilized (Vecton600, TMC Iberia), before pumping into mixing (n = 24) and respective experimental (n = 24, 50 l) tanks/RAS. To prevent fluctuations in environmental parameters, each RAS worked as a semi-closed system, with constant low flow external water input (flux > 2 l h^{-1}; 50 l tank turnover rate = 24 h). Consequently, ammonia (NH_3/NH_4^+), nitrite (NO_2^-) and nitrate (NO_3^-) concentrations were daily checked (Colourimetric kits, Aquamerk, Germany), and kept below detectable levels (i.e. NH_3/NH_4^+ < 0.25 mg l^{-1}; NO_2^- < 0.10 mg l^{-1}; NO_3^- < 0.20 mg l^{-1}), and salinity was kept at 35.0 ± 1.0 (V2 Refractometer, TMC Iberia, Portugal). Temperature and pH (multiparametric probe, Multi3420 SET G, WTW) were measured daily, directly in the holding tanks. Photoperiod was fixed at 12 h light:12 h dark.

As per experimental conditions, temperature in the tanks was down-regulated using chillers (±0.1 °C, Frimar, Fernando Ribeiro Lda), and up-regulated by submerged 200 W heaters (V2Therm, TMC Iberia). Seawater carbonate chemistry was altered through CO_2-enriched air input, with pH (8.0 and 7.5) used as proxy measurement. We used a Profilux system (±0.1, Profilux 3.1 N, GHL) as pH controller, connected to each tank by individual pH probes. Within each RAS, pH was down-regulated by injection of certified CO_2-enriched air (Air Liquide), and up-regulated by injection of atmospheric air. Seawater carbonate system speciation (Table S1) was calculated once every week from $pH_{total\ scale}$ (pH_T) and total alkalinity. pH_T was quantified via a Metrohm pH meter (826 pH mobile, Metrohm, Filderstadt, Germany) connected to a glass electrode (Schott IoLine, SI analytics, ±0.001) and calibrated against TRIS–HCl (TRIS) and 2-aminopyridine-HCl (AMP; Mare, Liège, Belgium) seawater buffers (Dickson et al., 2007). Total alkalinity was measured spectrophotometrically (wavelength = 595 nm; UV-1800 Shimadzu, Japan) through base neutralization by formic acid and a pH sensitive dye (bromophenol blue), following Sarazin et al. (1999). Total dissolved inorganic carbon (C_T), pCO_2 and aragonite saturation were calculated using CO2SYS software (Lewis and Wallace, 1998), with dissociation constants from Mehrbach et al. (1973) as refitted by Dickson and Millero (1987). The non-contaminated and contaminated fish were fed similar diets, differing only on MeHg content. Contaminated diet was fortified with MeHg (inserted in the form of MeHg(II) chloride, CH_3ClHg, 99.8%, Sigma-Aldrich, solubilized previously in ethanol). Given our dietary option, ecologically relevant MeHg concentrations (low contamination, ~0.12 mg kg^{-1} wet weight (ww); and high contamination, ~1.6 mg kg^{-1} ww) were chosen based on levels found in common juvenile *A. regius* prey species (mainly gastropods and crustaceans, particularly *Crangon crangon*) from contaminated coastal areas (Cabral and Ohmert, 2001; Cardoso et al., 2014; Nunes et al., 2008). The pellets given to fish allocated to non-contaminated and contaminated treatments had approximately 0.06 ± 0.01 mg kg^{-1} dry weight (dw) and 8.02 ± 0.01 mg kg^{-1} dw of MeHg, respectively, which were considered to mimick concentrations found in the field (see Maulvault et al., 2016, 2017). Feed composition, manufacturing and MeHg spiking processes were executed as described by Maulvault et al. (2016). Fish were fed two to three times a day and total feed quantity provided per day was approximately 1% (standard calculation for aquaculture) of animal weight (at the end of 30 days, each fish was given approximately 0.0106 mg of HgT). Selected feed quantity also minimized food remains, which, in case of existing, were siphoned together with fish faeces after feeding. Water samples were not taken as previous use of this feed showed no MeHg/Hg leakage into the water column (Maulvault et al., 2016).

After 15 days of lab acclimation (control conditions: 19 °C, CO_2 ≃ 400 μatm), fish were kept during 30 days under crossed-treatments of ocean warming (ΔT = 4 °C), acidification (ΔpH = 0.5 units, i.e. ΔpCO_2 = 1100 μatm) and MeHg contamination (contaminated and non-contaminated) in a full-factorial design, simulating predicted "business-as-usual" scenarios for the year 2100 (IPCC, 2014; Melzner et al., 2013; Schiedek et al., 2007). The experimental setup mimicked the design elaborated by Cornwall and Hurd (Fig. 3d, 2015). More specifically, the setup was divided in eight treatments (n = 3 tanks per treatment): i) 19 °C, 400 pCO_2 μatm (control conditions) and non-contaminated feed (MeHg: 0.06 mg kg^{-1}; HgT: 0.07 mg kg^{-1}), ii) 19 °C, 400 pCO_2 μatm and contaminated feed (MeHg: 8.02 mg kg^{-1}; HgT: 8.28 mg kg^{-1}), iii) 19 °C, 1500 pCO_2 μatm (control temperature and hypercapnic scenario) and non-contaminated feed (MeHg: 0.06 mg kg^{-1}; HgT: 0.07 mg kg^{-1}), iv) 19 °C, 1500 pCO_2 μatm and contaminated feed (MeHg: 8.02 mg kg^{-1}; HgT: 8.28 mg kg^{-1}); v) 23 °C, 400 pCO_2 μatm (warming and normocapnic scenario) and non-contaminated feed (MeHg: 0.06 mg kg^{-1}; HgT: 0.07 mg kg^{-1}); vi) 23 °C, 400 pCO_2 μatm and contaminated feed (MeHg: 8.02 mg kg^{-1}; HgT: 8.28 mg kg^{-1}); vii) 23 °C, 1500 pCO_2 μatm (warming and hypercapnic scenario) and non-contaminated feed (MeHg: 0.06 mg kg^{-1}; HgT: 0.07 mg kg^{-1}); and viii) 23 °C, 1500 pCO_2 μatm and contaminated feed (MeHg: 8.02 mg kg^{-1}; HgT: 8.28 mg kg^{-1}).

Survival rates were monitored throughout the experiment, and after 30 days fish were measured (total length) and weighed. Health status was assessed through the widely used Fulton's condition factor K (n = 6–8 per treatment), described by the following formula: $K = 100 \times (Weight / Length^3)$. Individuals were anesthetized with MS-222 and euthanized by swift spinal cord severing. Sample tissues of three organs (muscle, liver and gills) were harvested and frozen (−80 °C) until further analysis.

2.2. Total mercury and methylmercury accumulation

Methylmercury extraction from samples (fish and different feeds, n = 3–6) was performed as described by Scerbo and Barghigiani (1998), i.e. freeze-dried samples (~200 mg) were hydrolyzed in 10 ml of hydrobromic acid (47% w/w, Merck), following addition of 35 ml toluene (99.8% w/w, Merck) to allow MeHg extraction and removal with 6 ml cysteine solution (1% L-cysteinium chloride in 12.5% anhydrous sodium sulfate and 0.775% sodium acetate, Merck). Afterwards, HgT (all samples) and MeHg (feed samples) were determined (10–15 mg for solids or 100–200 μl for liquids) by atomic absorption spectrometry (AAS), following EPA (2007) by means of an automatic Hg analyser (AMA 254, LECO, USA). Mercury concentrations were calculated through linear calibration (using >5 standard concentrations), with a Hg(II) nitrate standard solution (1000 mg l^{-1}, Merck) dissolved in nitric acid (0.5 mol l^{-1}, Merck), reporting ~0.01 mg kg^{-1} and ~0.04 mg kg^{-1} as detection and quantification limits. Accuracy was further checked by analysing certified reference material DORM-4, and framing results obtained within the certified range of values (Table S2). A minimum of three measurements were performed per sample. Blanks were always tested in the same conditions as the samples and measurements were taken in triplicate. All laboratory ware was previously cleaned using nitric acid (20% v/v) for 24 h and ultrapure water, in that order. All standards and reagents were of analytical (pro analysis) or superior grade.

2.3. Enzymatic assays

2.3.1. Preparation of tissue extracts

Muscle, liver and gill samples (n = 4–6) were homogenized (Ultra-Turrax, Staufen, Germany) in accordance to body mass of each sample in

homogenization buffer, 300 mg tissue per 1 ml phosphate buffered saline solution (PBS, pH 7.4: 0.14 M NaCl, 2.7 mM KCl, 8.1 mM Na_2HPO_4, 1.47 mM KH_2PO_4). Homogenates were centrifuged (20 min at 14,000 rpm at 4 °C) and antioxidant enzyme activities, as well as lipid peroxidation and heat shock response concentrations, quantified in the supernatant fraction. All enzyme assays were tested with commercial enzymes obtained from Sigma-Aldrich (St. Louis, USA), and each sample was run in triplicate (technical replicates). The enzyme results were normalized with total protein content following the Bradford method (Bradford, 1976).

2.3.2. Lipid peroxides assay (malondialdehyde concentration)

As an end-product of oxidative stress, malondialdehyde (MDA) concentration was used as a proxy to assess extent of lipid peroxidation in the muscle. We used the thiobarbituric acid reactive substances (TBARS) protocol described by Uchiyama and Mihara (1978). A total of 10 μl of each sample were added to 45 μl of monobasic sodium phosphate buffer (50 mM), followed by addition of 12.5 μl of sodium dodecyl sulfate (8.1%), 93.5 μl of trichloroacetic acid (20%, pH = 3.5) and 93.5 μl of thiobarbituric acid (1%) to each microtube. Then, 50.5 μl of ultrapure water were added to this mixture and placed in a vortex for 30 s. A needle was used to puncture the lids and microtubes were incubated in boiling water (10 min) followed by ice cooling. Subsequently, 62.5 μl of ultrapure water and 312.5 μl of n-butanol pyridine (15:1, v/v) (Sigma-Aldrich, Hamburg, Germany) were added and microtubes centrifuged (5000 rpm; 5 min.). Afterwards, 150 μl of the supernatant's reaction were introduced into a 96-well microplate in duplicate and absorbance was read at 530 nm. Lipid peroxides (i.e., MDA concentration) were determined using malondialdehyde (dimethylacetal) (MDA) (Merck, Switzerland) standards in an eight-point calibration curve (0–0.3 μM). Results were expressed in relation to the sample total protein (nmol mg^{-1} total protein).

2.3.3. Catalase (CAT) activity

Catalase activity in the muscle was assessed through an adaptation of the method described by Johansson and Borg (1988). In this assay, 20 μl of each sample, 100 μl of 100 mM potassium phosphate and 30 μl of methanol were added to a 96-well microplate, which was promptly shaken and incubated for 20 min. Afterwards, 30 μl of potassium hydroxide (10 M KOH) and 30 μl of purpald (34.2 mM in 0.5 M HCl) were added to each well, and the plate shaken and incubated for another 10 min. Subsequently, 10 μl of potassium periodate (65.2 mM in 0.5 M KOH) was added to each well and a final incubation was performed for 5 min. Using a microplate reader (Asys UVM 340, Biochrom, USA), enzymatic activity was determined spectrophotometrically at 540 nm. Formaldehyde concentration of the samples was calculated based on a calibration curve (from 0 to 75 μM formaldehyde), followed by the calculation of CAT activity for each sample, where one unit of CAT is defined as the amount that will cause the formation of 1.0 nmol of formaldehyde per minute at 25 °C. The results are expressed in relation to total protein content (nmol min mg^{-1} protein).

2.3.4. Superoxide dismutase (SOD) activity

SOD activity in the muscle was determined following the nitro blue tetrazolium (NBT) method adapted from Sun et al. (1988). Superoxide radicals (O_2^-) are generated by xanthine oxidation, and simultaneous reduction of NBT to formazan. SOD competes with NBT for the dismutation of O_2^- into hydrogen peroxide (H_2O_2) and molecular oxygen, and this is used to determine enzyme activity. Briefly, the assay was performed using a 96-well microplate (Nunc-Roskilde), adding to each well 200 μl of 50 mM phosphate buffer (pH 8.0) (Sigma-Aldrich), 10 μl of 3 mM EDTA (Riedel-de Haën, Seelze, Germany), 10 μl of 3 mM xanthine (Sigma-Aldrich), 10 μl of 0.75 mM NBT (Sigma-Aldrich) and 10 μl of SOD standard or sample. Reaction began by adding 10 μl of 100 mU xanthine-oxidase (XOD, Sigma-Aldrich) and absorbance (560 nm) was recorded every 5 min for 25 min, using a plate reader (Asys UVM 340, Biochrom, USA). SOD from bovine erythrocytes (Sigma-Aldrich) was used as standard and positive control, and a negative control included all components except SOD or sample. The latter yielded a maximum threshold in absorbance, which allowed the assessment of inhibition percentage per minute (averaged from 25 min), which is caused by SOD activity. Thus, SOD activity percentage was expressed in % inhibition mg^{-1} of total protein.

2.3.5. Glutathione S-transferase (GST) activity

GST activity in the muscle was determined according to the procedure described by Habig et al. (1974) and optimized for 96-well microplate (Sigma Technical Bulletin, GST Assay Kit CS0410). In this assay, 1-chloro-2,4-dinitrobenzene (CDNB) is used as substrate and, upon conjugation of the thiol group of glutathione to the CDNB absorbance is proportionally increased, enabling spectrophotometric determination. The assay included 200 mM L-glutathione (reduced), 100 mM 1-chloro-2,4-dinitrobenzene (CDNB) solution and Dulbecco's PBS. Equine liver GST (Sigma-Aldrich) was used as positive control to validate the assay. Briefly, 180 μl of substrate solution were added to 20 μl sample in each well of a 96-well microplate (Nunc-Roskilde) and absorbance (at 340 nm) was registered every minute during 6 min, through a plate reader (Asys UVM 340, Biochrom, USA). Finally, GST activity was calculated using a molar extinction coefficient for CDNB of 5.3 εmM (Sigma Technical Bulletin, CS0410), as follows: GST activity = (ΔA340 min / 0.0053) × (Total volume / Sample volume) × dilution factor. Results were expressed in relation to total protein of the sample (nmol min mg^{-1} total protein).

2.3.6. Heat shock proteins

Heat shock protein (Hsp70/Hsc70) content in the muscle, liver and gills was assessed by Enzyme-Linked Immunoabsorbent Assay (ELISA) protocol adapted from Njemini et al. (2005). Specifically, 10 μl of the supernatant was diluted in 990 μl of PBS and 50 μl of that sample were added to a 96-well microplate (Microloan 600, Greiner) and allowed to incubate overnight at 4 °C. On the next day, microplates were washed (three times) in 0.05% PBS-Tween-20. 100 μl of blocking solution (1% bovine serum albumin (BSA) Sigma-Aldrich) were added to each well and left to incubate for 2 h at room temperature. After washing the 96-well plates, we introduced 50 μl of 5 μg ml^{-1} primary antibody (Mouse anti-Hsp70/Hsc70, Acris, San Diego, CA, USA), and again left incubating overnight at 4 °C. According to manufacturer details, this primary antibody (AM12032PU-N) possesses broad range reactivity, e.g. in varied fish species, making it suitable for our analysis. On the next

Table 1
GLM analysis of *A. regius* Fulton's K and total mercury (HgT) concentration in tissues (3 levels within contaminated treatments: liver, muscle and gills) exposed to MeHg contamination (2 levels: non-contaminated and contaminated) for 30 days. Model formula on top, family and respective model AIC in the bottom. Est – Estimates; Std Error – Standard Error. Bold values indicate $p < 0.05$. For more details please see the R script in Supplemental data.

	Est	Std Error	t value	p value
GLM: Fulton's K in function of MeHg				
(Intercept)	1.602	0.041	39.09	<**0.001**
MeHg	−0.072	0.057	0.057	0.213
Family = Gaussian			AIC = −8.6	
GLM: HgT in function of MeHg * tissues				
(Intercept)	1.576	0.082	19.11	<**0.001**
Muscle & gills	0.470	0.128	3.665	<**0.001**
Muscle & liver	0.660	0.130	5.063	<**0.001**
Gills & liver	0.191	0.141	1.355	0.181
Family = Gamma			AIC = 270.3	

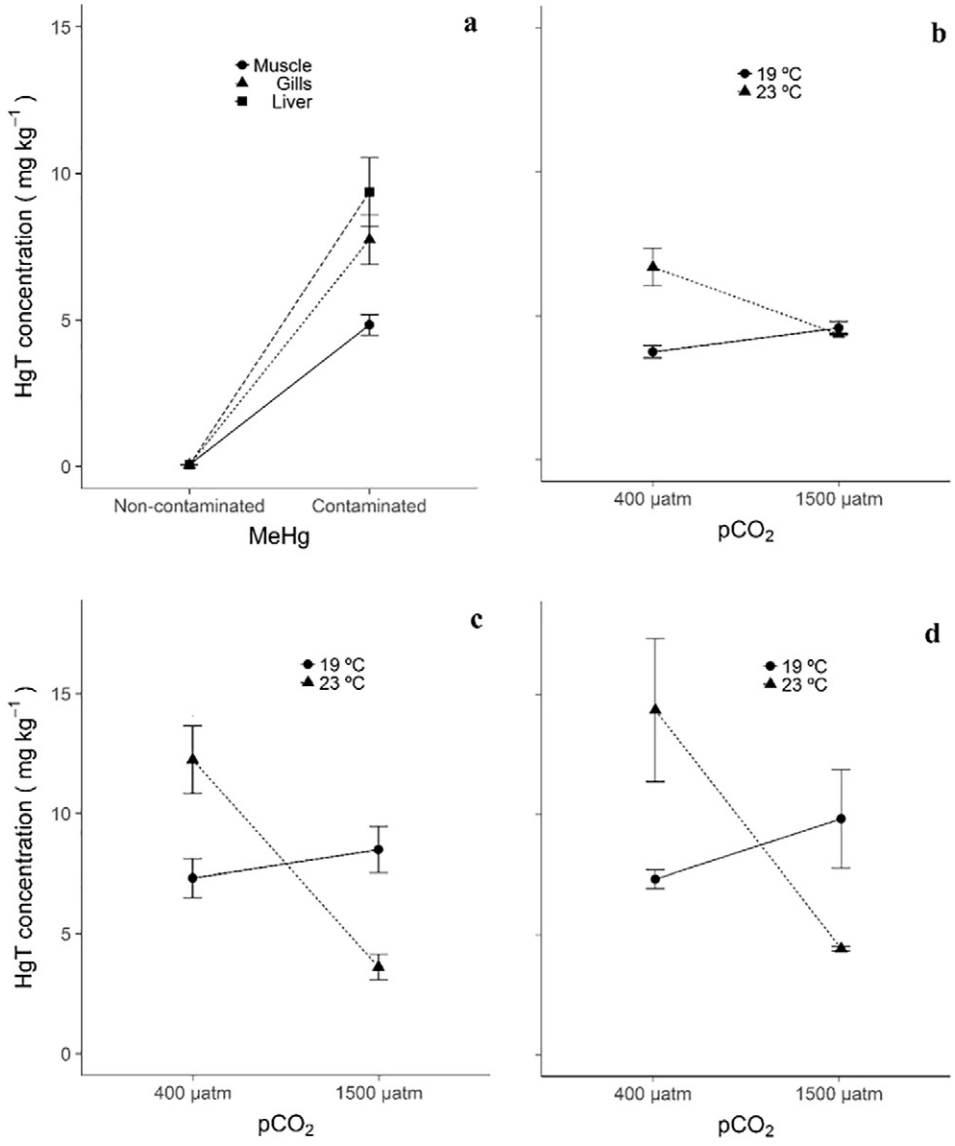

Fig. 1. Total mercury (HgT) accumulation (mean ± SE) in *A. regius*: a) differences among tissues (muscle, gills and liver); and shaped by interactions between temperature (19 and 23 °C) and CO_2 (400 and 1500 µatm) within b) muscle, c) gills and d) liver, respectively. Graphs were plotted according to significant factors yielded by GLM analysis described in Tables 1 and 2, respectively.

day, the non-linked antibody was removed by washing the microplates, and 50 µl of 1 µg ml^{-1} of the secondary antibody, antimouse IgC, Fab specific, alkaline phosphatase conjugate (Sigma-Aldrich) were added and incubated for 2 h at room temperature. After three additional washes, 100 µl of substrate (SIGMA FASTTM *p*-Nitrophenyl Phosphate Tablets, Sigma-Aldrich) was added to each well and incubated 10–30 min at room temperature. Stop solution (50 µl; 3 N NaOH) was added in each well, and absorbance was read at 405 nm in a 96-well microplate reader (Asys UVM 340, Biochrom, USA). The amount of Hsp70/Hsc70 present in the samples was calculated from an absorbance/concentration calibration curve based on serial dilutions of purified Hsp70 active protein (Acris), ranging from 0 to 2000 ng ml^{-1}. The coefficients of variation were below 2.5% and results were expressed in relation to the sample total protein (ng mg^{-1} total protein).

Table 2
GLM analysis of total mercury concentration (HgT) within each sampled tissue (liver, muscle and gills) of *A. regius* exposed to MeHg for 30 days, under crossed treatments of temperature (T, 2 levels: 19 °C and 23 °C) and CO_2 (CO_2, 2 levels: 400 µatm and 1500 µatm). Model formula on top, family and respective model AIC in the bottom. Est – Estimates; Std Error – Standard Error. Bold values indicate $p < 0.05$. For more details please see the R script in Supplemental data.

	GLM: liver HgT in function of T * CO_2				GLM: muscle HgT in function of T * CO_2				GLM: gills HgT in function of T * CO_2			
	Est	Std Error	t value	p value	Est	Std Error	t value	p value	Est	Std Error	t value	p value
(Intercept)	2.287	0.151	15.18	<**0.001**	1.520	0.063	24.31	<**0.001**	2.059	0.125	16.74	<**0.001**
T	0.794	0.261	−3.043	**0.010**	0.579	0.088	6.551	<**0.001**	−0.917	0.191	−4.792	<**0.001**
CO_2	−0.295	0.195	−1.514	0.156	−0.201	0.088	−2.268	**0.035**	−0.157	0.162	−0.970	0.350
T * CO_2	1.468	0.326	4.508	<**0.001**	0.627	0.125	5.017	<**0.001**	1.452	0.251	5.799	<**0.001**
Family = Gamma (all)			AIC = 82.0				AIC = 59.8				AIC = 73.3	

2.4. Statistics

All statistical analyses were performed on R Studio (R Development Core Team, 2016). We used Generalized Linear Models (GLM) analysis to infer significant differences between sampled groups (see R script provided in the Supplemental data for a step-by-step protocol). Mix models, e.g. tank as random factor, were ruled unnecessary as previous analysis (using 'lme4' and 'nlme' packages) showed no significant differences between tanks, within each group treatment, for all variables used. Best model selection fit for our data was found using the Akaike Information Criterion (AIC), a widespread indicator that balances model complexity with model quality of fitness (Quinn and Keough, 2002). Thus, models were simplified and factors that did not influence data variation were removed. Data was fitted using Gaussian family and model residuals were checked for homogeneity of variances, independence and leverage to validate final models. When assumptions were not met, we turned to gamma family models to fit our data, and model validation was assessed following the same procedure. Temperature (T, 2 levels: 19 °C, 23 °C) CO_2 (CO_2, 2 levels: 400 μatm, 1500 μatm), MeHg exposure (MeHg, 2 levels: Non-contaminated, 0.06 mg kg^{-1}; Contaminated, 8.02 mg kg^{-1}) and organ tissue sampled (Tissue, 3 levels: Muscle, Gills, Liver) were generally used as explanatory variables or factors, according to each specific dependent variable. Finally, ANOVA tests were used to provide F and p values for factors with more than two levels.

3. Results

After 30 days of exposure, no mortalities were registered in any treatment. Moreover, Fulton condition (K) did not show any significant differences between treatments (MeHg, $p > 0.05$, GLM analysis in Table 1). Regarding total mercury (Hg) concentrations, contaminated and non-contaminated scenarios were significantly different (GLM analysis, $t = 9.079$, $p < 0.001$, see Supplemental data) and Hg accumulation was also tissue-specific (ANOVA F test, $F = 14.015$, $p < 0.001$, see Supplemental data). Among tissues, Hg concentration was lower in the muscle than in other organs analysed (Muscle & Liver/Muscle & Gills, $p < 0.001$, GLM Analysis in Table 1, Fig. 1a). In addition, consistent in all tissues tested, temperature and high CO_2 interactively affected MeHg accumulation ($T \times CO_2$, $p < 0.001$ for all tissues, GLM analysis in Table 2, Fig. 1b–d), showing an antagonistic relation. That is, while temperature increased Hg accumulation, this stimulating effect was offset by high CO_2.

Lipid peroxidation and oxidative stress response were measured in the muscle, the largest tissue. A significant additive effect between increasing temperature and MeHg contamination was detected, causing MDA build-up ($T \times$ MeHg, $p < 0.05$, GLM analysis in Table 3, Fig. 2). Regarding the antioxidant enzyme machinery response, CAT activity was only increased by MeHg contamination (MeHg, $p < 0.05$, GLM analysis in Table 4, Fig. 3a). On the other hand, isolated high temperature- or CO_2-related increases in SOD activity were reversed when both stressors co-occurred ($T \times CO_2$, $p < 0.001$, GLM analysis in Table 4, Fig. 3b). Finally, GST activity was modelled by two interactions between CO_2 and temperature ($T \times CO_2$, $p < 0.05$, GLM analysis in Table 4, Fig. 4a), and between CO_2 and MeHg contamination ($CO_2 \times$ MeHg, $p < 0.01$, GLM analysis in Table 4, Fig. 4b). In both cases, increased CO_2 inhibited GST activity when combined with warming (Fig. 4a) or MeHg contamination (Fig. 4b).

Heat shock response was differently affected by stressors within tissues (ANOVA F test, $F = 11.732$, $p < 0.001$, see Supplemental data). Hsp70 production reported higher levels in the liver and lower in the gills (liver > muscle > gills; see GLM analysis in Table 5 for p values, Fig. 5a). Looking at tissue-specific effects, Hsp70 concentration was positively affected by MeHg contamination within the gills (Gills, $p < 0.05$, GLM analysis in Table 5, Fig. 5b). On the other hand, temperature and CO_2 interactively modulated Hsp70 production in the muscle ($T \times CO_2$, $p < 0.001$, GLM analysis in Table 5, Fig. 5c), with temperature-stimulated Hsp70 production being dampened by co-occurring high CO_2. Likewise in the liver, MeHg contamination increased Hsp70 production, but this effect was countered by increased CO_2 ($CO_2 \times$ MeHg, $p < 0.01$, GLM analysis in Table 5, Fig. 5d).

Table 3
GLM analysis of malondialdehyde (MDA) build-up in *A. regius* after 30 days exposed to crossed treatments of MeHg contamination (MeHg, 2 levels, non-contaminated and contaminated) and temperature (T, 2 levels: 19 °C and 23 °C). Model formula on top, family and respective model AIC in the bottom. Est – Estimates; Std Error – Standard Error. Bold values indicate $p < 0.05$. For more details please see the R script in Supplemental data.

	Est	Std Error	t value	p
GLM: MDA in function of T * MeHg				
(Intercept)	0.026	0.003	8.055	<**0.001**
T	−0.010	0.005	−2.163	**0.036**
MeHg	−0.004	0.005	−0.954	0.345
T * MeHg	0.014	0.007	2.174	**0.035**
Family = Gaussian			AIC = −277.2	

4. Discussion

4.1. Non-lethal preferential accumulation

The present study showed that Hg contamination, ocean warming and acidification interactively affected fish physiology at sublethal levels, i.e. zero mortality and no effects on Fulton condition were registered. The fact that the meagre (*A. regius*) is a very resilient species and easily adapts to environmental change (Monfort, 2010) may explain the absence of effects at these specific levels, after a short-term acclimation.

After 30 days of exposure to MeHg contaminated feed, mean levels of Hg accumulation (HgT concentrations up to 12–13 mg kg^{-1} dry weight) found in *A. regius* were similar to those reported in other coastal teleost fish under similar experimental conditions, such as in the temperate sole *Solea senegalensis* (Sampaio et al., 2016) and the seabass

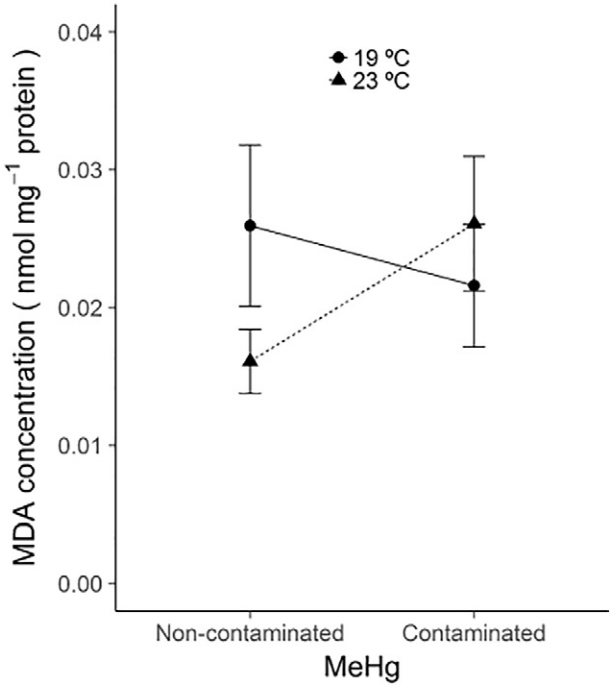

Fig. 2. Malondialdehyde (MDA) build-up concentrations (mean ± SE) in *A. regius* muscle driven by an interaction between MeHg contamination (Non-contaminated and contaminated) and temperature (19 and 23 °C). Graphs were plotted according to significant factors yielded by GLM analysis described in Tables 3 and 4, respectively.

Table 4
GLM analysis of oxidative stress response (CAT, SOD and GST) in *A. regius* after 30 days exposed to crossed treatments of MeHg exposure (MeHg, 2 levels: non-contaminated and contaminated), temperature (T, 2 levels: 19 °C and 23 °C) and CO_2 (CO_2, 2 levels: 400 μatm and 1500 μatm). Model formula on top, family and respective model AIC in the bottom. Est – Estimates; Std Error – Standard Error. Bold values indicate $p < 0.05$. For more details please see the R script in Supplemental data.

	Est	Std Error	t value	p
GLM: CAT in function of $CO_2 * MeHg$				
(Intercept)	4.375	0.399	10.96	<**0.001**
CO_2	−0.454	0.564	−0.804	0.426
MeHg	1.482	0.564	2.625	**0.012**
$CO_2 * MeHg$	1.313	0.818	1.605	0.116
Family = Gaussian			AIC = 166.2	
GLM: SOD in function of $CO_2 * T + CO_2 * MeHg$				
(Intercept)	9.496	1.040	9.135	<**0.001**
T	3.346	1.200	−2.787	**0.008**
CO_2	−1.264	1.484	−0.852	0.399
MeHg	1.614	1.200	1.344	0.186
$T * CO_2$	6.319	1.744	3.623	<**0.001**
$CO_2 * MeHg$	−3.399	1.744	−1.949	0.058
Family = Gaussian			AIC = 237.3	
GLM: GST in function of $T * CO_2 * MeHg$				
(Intercept)	7.561	0.676	11.19	<**0.001**
T	−1.174	0.955	−1.229	0.227
CO_2	−2.320	0.955	−2.428	**0.020**
MeHg	−2.054	0.955	−2.150	**0.038**
$T * CO_2$	4.076	1.351	3.017	**0.005**
T * MeHg	2.375	1.351	1.758	0.087
CO2 * MeHg	4.427	1.351	3.277	**0.002**
$T * CO_2 * MeHg$	−3.422	1.970	−1.737	0.090
Family = Gaussian			AIC = 186.1	

Dicentrarchus labrax (Maulvault et al., 2016). Affinity for metal accumulation varied between fish tissues with increasing Hg accumulation as follows: muscle < gills < liver, which is in line with previous reports on mercury tissue preferential accumulation (Gonzalez et al., 2005; Korbas et al., 2012). Specifically, due to its high lipophilicity, Hg accumulates preferentially in lipid-rich organs, such as the brain or the liver (Guzzi and La Porta, 2008). Thus, the muscle is a tissue generally characterized for its low metal affinity (Jezierska and Witeska, 2006) compared to, e.g. the liver, where metals also accumulate at higher levels, due to its key role in metal accumulation and detoxification (Gbem et al., 2001; Gonzalez et al., 2005; Wagner and Boman, 2003). Furthermore, as a consequence of increased blood supply, the gills are organs likewise known to possess higher Hg affinity than the muscle (Jezierska and Witeska, 2006; Vergilio et al., 2012).

4.2. Environmental influence on mercury accumulation

Mercury accumulation in fish is known to depend on the water physicochemical properties (e.g. temperature, pH, and alkalinity) (Harris and Bodaly, 1998; Ponce and Bloom, 1991; Wren et al., 1991). Confirming previous reports (Dijkstra et al., 2013; Maulvault et al., 2016), our results showed a consistent increase in Hg accumulation under the warming scenario. Most likely, temperature increases Hg bioaccumulation in fish due to enhanced metabolism and consequent higher intake of MeHg-contaminated prey (Dijkstra et al., 2013; MacLeod and Pessah, 1973). However, when both temperature and CO_2 stressors were present, Hg accumulation was decreased. Despite previous evidence that lowered pH (<7.0 units) increases Hg accumulation in freshwater fish (Haines et al., 1992; Ponce and Bloom, 1991), the current findings do not reflect this pattern, arguably due to the magnitude of pH decrease (here we used pH 7.5). Instead, our results support recent studies demonstrating that hypercapnia dampens Hg accumulation in marine organisms (Li et al., 2017; Sampaio et al., 2016; Wang et al., 2017). There are several possible reasons which may mechanistically explain how an increase of H^+/CO_2 could lead to slower Hg accumulation rates via digestive system, mainly encompassing direct molecular mechanisms (competition between Hg and H^+ ions for binding sites, impacts on Hg plasma transport, lower phospholipidic membrane permeability, etc.) and alterations in the digestive system (reduced digestive efficiency, reduced uptake through the gut membrane, increased Hg depuration, among others) (Li et al., 2017). Indirectly, taking into account that the occurrence of both warming and acidification changes physiological thresholds (Christensen et al., 2011; Harley et al., 2006; Rosa et al., 2013; Rosa and Seibel, 2008; Sampaio et al., 2017), a degree of metabolic depression, and consequently less feed intake, is likely to play a role in decreased HgT accumulation (Dijkstra et al., 2013; Sampaio et al., 2016). Whatever the proximate mechanisms, CO_2-decreased Hg accumulation rates (and possibly the respective toxic effects; Li et al., 2017) in a pelagic predator, may translate into lower Hg transference and overall diminished biomagnification through the trophic chain in coastal ecosystems. From a consumer perspective, the counteracting CO_2 effect (hampering warming-stimulated Hg accumulation) was consistent in the muscle, the main tissue ingested by human population. Since this is the most

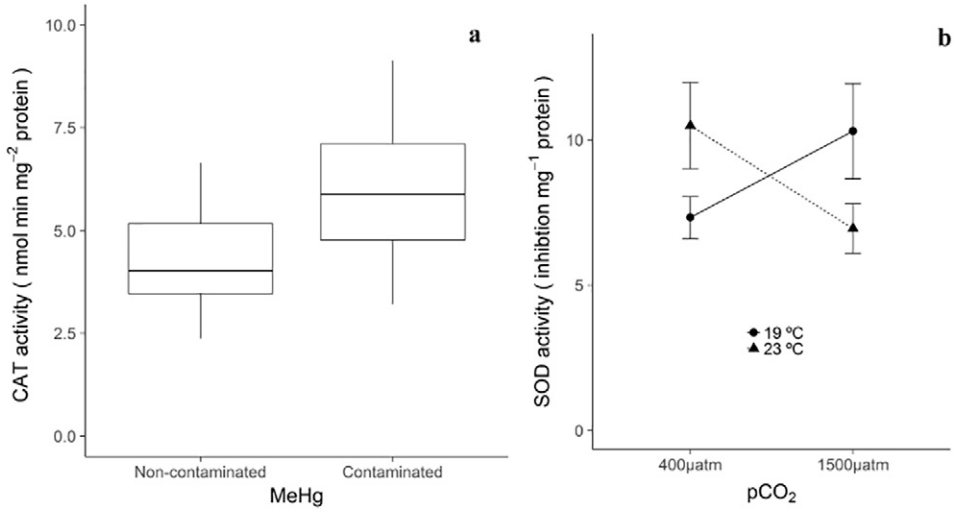

Fig. 3. a) Catalase (CAT) enzyme activities (mean ± SE) driven by MeHg contamination (Non-contaminated and Contaminated). b) Superoxide dismutase (SOD) activities (mean ± SE) in *A. regius* muscle driven by an interaction temperature (19 and 23 °C) and CO_2 (400 and 1500 μatm). Graphs were plotted according to significant factors yielded by GLM analysis described in Table 4.

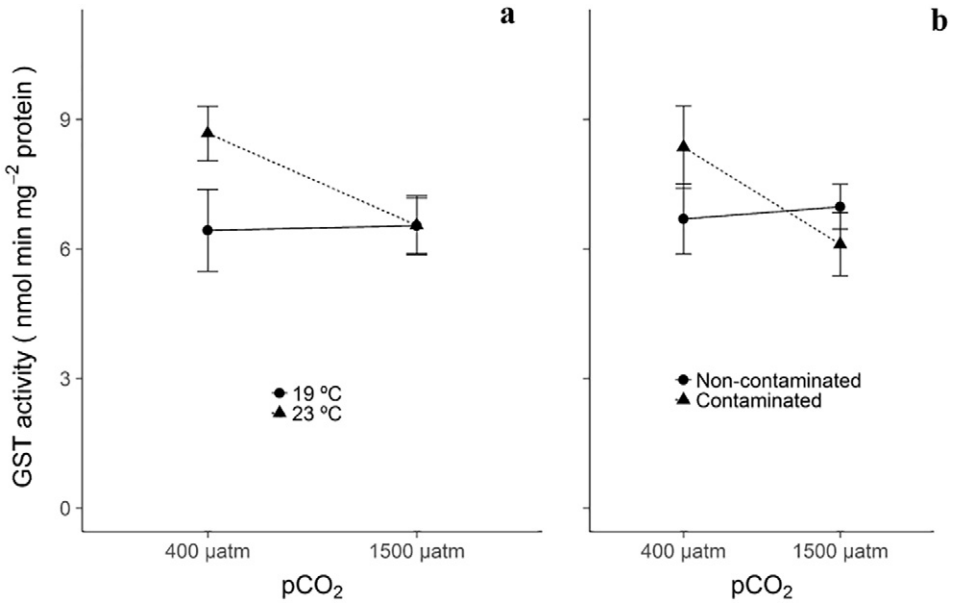

Fig. 4. Glutathione *S*-transferase (GST) activities (mean ± SE) in *A. regius* muscle driven by: a) an interaction between temperature (19 and 23 °C) and CO_2 (400 and 1500 µatm); and b) an interaction between MeHg contamination (non-contaminated and contaminated) and CO_2 (400 and 1500 µatm). Graphs were plotted according to significant factors yielded by GLM analysis (triple interaction) described in Table 4.

relevant tissue for commercialization, such results constitute an important finding in the seafood safety research area, warranting further investigation.

4.3. Oxidative stress under a multi-stressor environment

Exposure to MeHg contamination, ocean warming and acidification potentiated significant changes in meagre physiology. As expected from the results of previous studies in fish and other animal models (e.g. bivalves), lipid peroxidation and consequent MDA build-up was increased by the combined effects of contamination (in this case, MeHg) and increased temperature (Lannig et al., 2006; Pimentel et al., 2015; Sokolova and Lannig, 2008). Despite the capability of *A. regius* to overcompensate for temperature-elicited ROS, the further crippling of antioxidant defenses induced by contaminants, leads to oxidative damage (Sokolova and Lannig, 2008). However, the fact that simultaneous contamination and warming elicited only a small MDA build-up relatively to what has been reported for *Salmo salar* or *Dicentrarchus labrax* (Berntssen et al., 2003; Lannig et al., 2006; Pimentel et al., 2015), may be attributed to *A. regius* being a highly resilient estuarine species, i.e. possessing great tolerance to environmental stressors (Monfort, 2010). Further proof of *A. regius* resilience can be extracted from the fact that CO_2 did not elicit MDA production, in opposition to what has been verified for other temperate and tropical fish, albeit in different life stages (Pimentel et al., 2015; Rosa et al., 2016). Moreover, to cope with oxidative stress prompted by mercury contamination and warming, *A. regius* upregulated activities of the antioxidant enzymes CAT, SOD and GST, which is in line with previous studies reporting an overall enhanced antioxidative stress response to these stressors, in coastal fish (Maulvault et al., 2017; Pimentel et al., 2015; Vieira et al., 2009). While it is worth mentioning that increased CO_2 played a minor role in CAT activity (non-significant, MeHg * CO_2, $p = 0.116$), regarding the other enzymes, hypercapnia as a sole stressor generally provoked slight increases of antioxidant activity, as has been physiologically predicted (Dean, 2010) and empirically reported in, e.g. *Solea senegalensis* (Pimentel et al., 2015). However, when combined with other stressors, elevated CO_2 antagonized the co-occurring stressor effect (i.e. contamination and/or warming). In copepods, increased CO_2 (co-occurring with Hg contamination) upregulates the lysosome-autophagy pathway, which is responsible for removing damaged proteins and organelles, and effectively reduces oxidative stress (Li et al., 2017; Wang et al., 2017). Given that lysosomes and this biochemical pathway are conserved in nearly all animal cells (e.g. Kroemer and Jäättelä, 2005), this removal mechanism can potentially be activated in teleost fish, and may contribute to alleviate not only Hg induced stress, but also warming-related oxidative stress. Moreover, this antagonistic relation can also be explained by a CO_2-related increase of H^+ ion concentrations in the blood and cellular surroundings,

Table 5
GLM analysis of heat shock protein 70 (Hsp70) production in *A. regius* tissues (gills, muscle and liver) and, posteriorly within tissues, under crossed treatments of MeHg exposure (MeHg, 2 levels, non-contaminated and contaminated), temperature (T, 2 levels: 19 °C and 23 °C) and CO_2 (CO_2, 2 levels: 400 µatm and 1500 µatm). Model formula on top, family and respective model AIC in the bottom. Est – Estimates; Std Error – Standard Error. Bold values indicate $p < 0.05$. For more details please see the R script in Supplemental data.

	Est	Std Error	t value	p
GLM: Hsp70 in function of tissues				
(Intercept)	3.605	0.235	15.32	<**0.001**
Gills & liver	1.607	0.335	4.804	<**0.001**
Gills & muscle	0.975	0.333	2.929	**0.004**
Muscle & liver	0.633	0.335	1.890	0.061
Family = Gaussian			AIC = 481.5	
GLM: gills Hsp70 in function of T + MeHg				
(Intercept)	3.561	0.255	13.99	<**0.001**
T	−0.530	0.299	−1.775	0.083
MeHg	0.622	0.299	2.085	**0.043**
Family = Gaussian			AIC = 146.4	
GLM: muscle Hsp70 in function of T * CO_2				
(Intercept)	4.671	0.291	16.07	<**0.001**
T	−0.294	0.411	−0.715	0.479
CO_2	−0.955	0.411	−2.323	**0.025**
T * CO_2	−2.331	0.596	3.913	<**0.001**
Family = Gaussian			AIC = 137.0	
GLM: liver Hsp70 in function of T + CO_2				
(Intercept)	5.376	0.593	9.064	<**0.001**
CO_2	−0.588	0.839	−0.702	0.487
MeHg	1.315	0.839	−1.567	0.125
CO_2 * MeHg	3.627	1.235	2.938	**0.005**
Family = Gaussian			AIC = 73.3	

counterbalanced by bicarbonate increase (acid-base compensation) to normalize pH levels (Heuer and Grosell, 2014; Michaelidis et al., 2007). By itself, the presence of excessive H^+ ions activate free radical neutralizing defenses (Tiedke et al., 2013), which is in line with the present findings when hypercapnia acted as a sole stressor. However, the production of O_2^- and other ROS free radicals (e.g. OH^-) by other stressors may result in facilitated H_2O and H_2O_2 formation, due to chemical reactions balancing equilibrium (e.g. $H^+ + OH^- \rightleftharpoons H_2O$), thus eliminating free radicals and decreasing activity of antioxidant enzymes to basal standards.

4.4. Protein chaperone functioning under a multi-stressor environment

Hsp70 response was tissue-dependent, showing a pattern similar to HgT tissue preferential accumulation (liver showing higher levels, see first section), and what has been reported in other studies in marine organisms (Maulvault et al., 2017; Sokolova and Lannig, 2008). Comparatively to other tissues, high liver expression is to be expected given the fact that this organ plays a key role in metal accumulation and detoxification (Gbem et al., 2001; Wagner and Boman, 2003). Conversely, lower Hsp70 production verified in the gills may reflect the fact that exposure to contamination was not performed via water, but via feed, since this tissue is usually reactive to waterborne contaminants (see Feder and Hofmann, 1999). According to previous studies, protein chaperone functioning was activated under warming or Hg contamination, simultaneously with upregulation of antioxidant enzymes, which confirms that Hsp70 expression is closely correlated with other forms of antioxidative response (CAT, SOD, and GST) (Lesser, 2006; Iwama et al., 1998; Rosa et al., 2012, 2014a; Pimentel et al., 2015). More importantly, regarding interactions among stressors, and as observed for the antioxidant stress enzymatic machinery, hypercapnia revealed the same antagonistic relationship with other stressor's effects: increased CO_2 down-regulated heat shock response in the liver of contaminated fish and in the muscle of temperature-elevated fish. More so than for oxidative stress, the enhanced removal of damaged proteins and enzymes indirectly promoted by increased CO_2 (via up-regulated lysosome-autophagy) may have especially contributed to subside protein chaperone production. Given that Hsp70 production can also be stimulated by high ionic (e.g. H^+) concentrations (see Dean, 2010; Feder and Hofmann, 1999), we reason that the same additional mechanism by which hypercapnia potentially modulates oxidative stress can be applied for heat shock response. Enhanced CO_2 leads to increased H^+ concentration triggering physiological stress responses, while the facilitated conversion of free ions and radicals (H^+ and O-associated molecules) into H_2O and H_2O_2 leads to reduced stress input by warming, contamination, and hypercapnia (itself). Such regulation of key components of fish physiological stress response (antioxidant and protein chaperone responses), indicates that ocean acidification potentially suppresses the deleterious effects caused by co-occurring stressors, as has been reported for other marine organisms (e.g. copepods; Li et al., 2017).

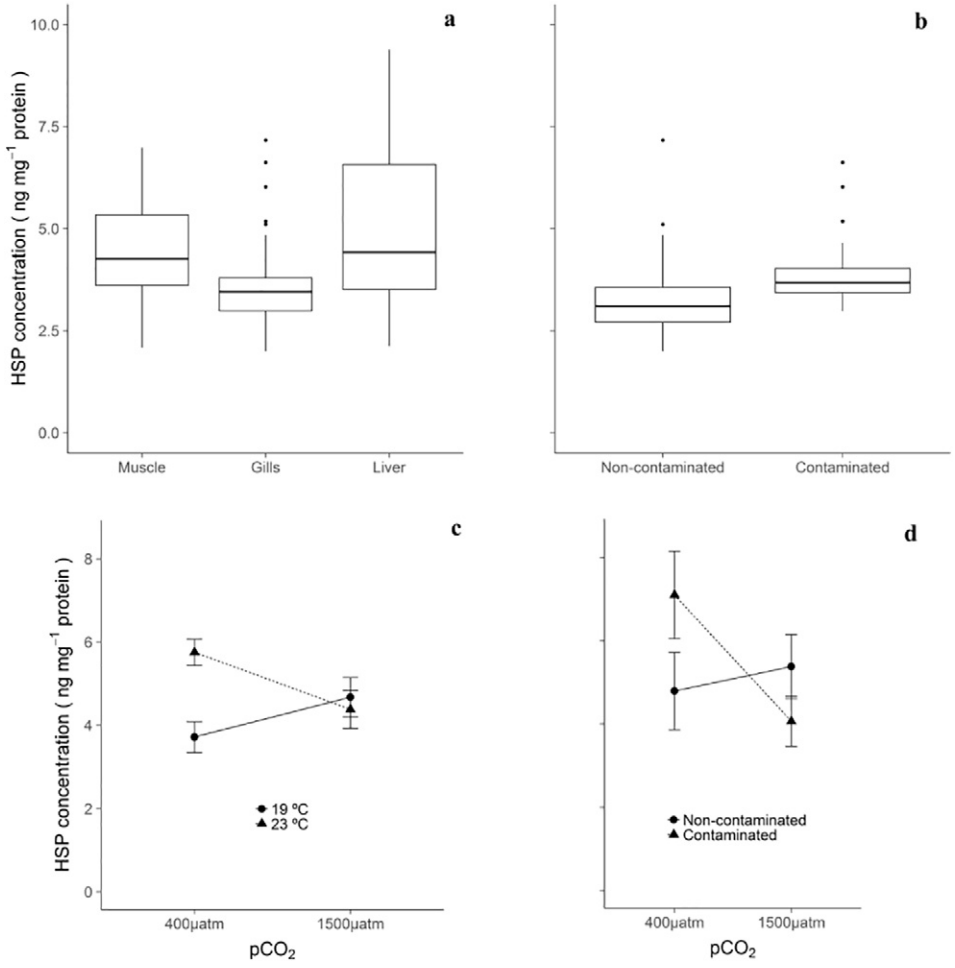

Fig. 5. Heat shock protein70 (Hsp70) concentrations (mean ± SE) in *A. regius*: a) tissues; b) in the gills shaped by MeHg contamination (Non-contaminated and Contaminated) and CO_2 (400 and 1500 µatm); in the c) muscle shaped by an interaction between temperature (19 and 23 °C) and CO_2 (400 and 1500 µatm); and in the d) liver shaped by an interaction between MeHg contamination (non-contaminated and Contaminated) and CO_2 (400 and 1500 µatm). Graphs were plotted according to significant factors yielded by GLM analysis described in Table 5.

5. Conclusions

In this study, we observed that sublethal MeHg contamination is organ selective (accumulating preferentially in the liver, across the organs analysed) and found that future abiotic conditions modulate its accumulation throughout the organism. In general, warming conditions enhanced MeHg accumulation but CO_2-linked impacts countered this effect. Likewise, despite negative effects as a sole stressor, acidification consistently elicited antagonistic responses to temperature and contamination impacts on oxidative stress (including heat shock response). These responses are potentially underpinned on stimulated removal of damaged proteins and organelles (Wang et al., 2017), as well as by the coinciding increase of hydrogen (H^+) and reactive oxygen species (e.g. O_2^-, OH^-) due to the spontaneous equilibrium of chemical reactions (e.g. $H^+ + OH^- \rightleftharpoons H_2O$) and consequent ROS elimination. Thus, for the first time in teleost fish, we found evidence that, when co-occurring with other stressors, ocean acidification can simultaneously diminish heavy metal (Hg specifically) accumulation and its toxic effects, as well as the physiological stress response elicited by both Hg and ocean warming. Ultimately, not only may these dampening effects translate into diminished contaminant biomagnification within the trophic chain, but also contribute to balancing fish physiology and promote homeostasis.

In the future, it is important to deepen our understanding on the mechanisms underlying this antagonistic relationship between acidification and other stressors, and evaluate its presence in other species, particularly less-resilient ones. Further knowledge on climate change and contamination impacts on fish ecophysiology (specifically, biochemical stress-coping mechanisms and response-activated pathways) will help towards better comprehension of future fish stock health conditions and forecasting socio-ecological consequences in the oceans of tomorrow. Further multi-stressor studies on seafood safety and biochemical changes should follow, with the intent of assisting stakeholders and regulatory authorities to define future consumption recommendations and preventive legislation.

Acknowledgments

We thank Kenneth Storey for the helpful discussion and IPMA-Olhão for providing juvenile meagre specimens for the trials. This work was supported by Fundação para a Ciência e a Tecnologia (FCT): PhD (ES, SFRH/BD/131771/2017; ARL, SFRH/BD/97070/2013; JRP, SFRH/BD/111153/2015; ALM, SFRH/BD/103569/2014) and post-doctoral (TFG, SFRH/BPD/98590/2013; TR, SFRH/BPD/98590/2013) grants, as well as RR and AM in the framework of the IF2013 and IF2014 programs.

Appendix A. Supplementary data

Supplementary data to this article can be found online at https://doi.org/10.1016/j.scitotenv.2017.11.059.

References

Anacleto, P., Luísa, A., Lopes, V.M., Repolho, T., Diniz, M., Leonor, M., Marques, A., Rosa, R., 2014. Comparative biochemistry and physiology, part a ecophysiology of native and alien-invasive clams in an ocean warming context. Comp. Biochem. Physiol. A 175: 28–37. https://doi.org/10.1016/j.cbpa.2014.05.003.

Berntssen, M.H.G., Aatland, A., Handy, R.D., 2003. Chronic dietary mercury exposure causes oxidative stress, brain lesions, and altered behaviour in Atlantic salmon (*Salmo salar*) parr. Aquat. Toxicol. 65 (1), 55–72.

Bradford, M.M., 1976. A rapid and sensitive method for the quantitation of microgram quantities of protein utilizing the principle of protein-dye binding. Anal. Biochem. 72:248–254. https://doi.org/10.1016/0003-2697(76)90527-3.

Burger, J., Dixon, C., Boring, S., Gochfeld, M., 2003. Effect of deep-frying fish on risk from mercury. J. Toxicol. Environ. Health A 66 (9), 817–828.

Cabral, H.N., Ohmert, B., 2001. Diet of juvenile meagre, *Argyrosomus regius*, within the Tagus estuary. Cah. Biol. Mar. 42 (3), 289–293.

Campbell, L.M., Norstrom, R.J., Hobson, K.A., Muir, D.C.G., Backus, S., Fisk, A.T., 2005. Mercury and other trace elements in a pelagic Arctic marine food web (Northwater Polynya, Baffin Bay). Sci. Total Environ. 351, 247–263.

Cardoso, P.G., Pereira, E., Duarte, A.C., Azeiteiro, U.M., 2014. Temporal characterization of mercury accumulation at different trophic levels and implications for metal biomagnification along a coastal food web. Mar. Pollut. Bull. 87 (1):39–47. https://doi.org/10.1016/j.marpolbul.2014.08.013.

Christensen, A.B., Nguyen, H.D., Byrne, M., 2011. Thermotolerance and the effects of hypercapnia on the metabolic rate of the ophiuroid *Ophionereis schayeri*: inferences for survivorship in a changing ocean. J. Exp. Mar. Biol. Ecol. 403 (1–2):31–38. https://doi.org/10.1016/j.jembe.2011.04.002.

Coccini, T., Randine, G., Candura, S.M., Nappi, R.E., Prockop, L.D., Manzo, L., 2000. Low-level exposure to methylmercury modifies muscarinic cholinergic receptor binding characteristics in rat brain and lymphocytes: physiologic implications and new opportunities in biologic monitoring. Environ. Health Perspect. 108 (1):29–33. https://doi.org/10.2307/3454292.

Cornwall, C.E., Hurd, C.L., 2015. Experimental design in ocean acidification research: problems and solutions. ICES J. Mar. Sci. 73, 572–581.

Dean, J.B., 2010. Hypercapnia causes cellular oxidation and nitrosation in addition to acidosis: implications for CO_2 chemoreceptor function and dysfunction. J. Appl. Physiol. 108 (6):1786–1795. https://doi.org/10.1152/japplphysiol.01337.2009.

Dickson, A., Millero, F., 1987. A comparison of the equilibrium constants for the dissociation of carbonic acid in seawater media. Deep-Sea Res. 34, 1733–1743.

Dickson, A.G., Sabine, C.L., Christian, J.R., 2007. Guide to best practices for ocean CO_2 measurements. PICES Special Publication 3.

Dijkstra, J.A., Buckman, K.L., Ward, D., Evans, D.W., Dionne, M., Chen, C.Y., 2013. Experimental and natural warming elevates mercury concentrations in estuarine fish. PLoS One 8 (3):1–9. https://doi.org/10.1371/journal.pone.0058401.

Dorts, J., Kestemont, P., Thézenas, M.-L., Raes, M., Silvestre, F., 2014. Effects of cadmium exposure on the gill proteome of *Cottus gobio*: modulatory effects of prior thermal acclimation. Aquat. Toxicol. 154, 87–96.

Durrieu, G., Maury-Brachet, R., Girardin, M., Rochard, E., Boudou, A., 2005. Contamination by heavy metals (Cd, Zn, Cu, and Hg) of eight fish species in the Gironde estuary (France). Estuaries 28 (4):581–591. https://doi.org/10.1007/BF02696069.

EPA, 2007. Method 7473 Mercury in Solids and Solutions by Thermal Decomposition, Amalgamation, and Atomic Absorption Spectrophotometry. U.S. Environmental Protection Agency.

Evers, D.C., Wiener, J.G., Basu, N., Bodaly, R.A., Morrison, H.A., Williams, K.A., 2011. Mercury in the Great Lakes region: bioaccumulation, spatiotemporal patterns, ecological risks, and policy. Ecotoxicology 20 (7), 1487–1499.

Feder, M.E., Hofmann, G.E., 1999. Heat-shock proteins, molecular chaperones, and the stress response: evolutionary and ecological physiology. Annu. Rev. Physiol. 61: 243–282. https://doi.org/10.1146/annurev.physiol.61.1.243.

Fonseca, V.F., França, S., Serafim, A., Company, R., Lopes, B., Bebianno, M.J., Cabral, H.N., 2011. Multi-biomarker responses to estuarine habitat contamination in three fish species: *Dicentrarchus labrax*, *Solea senegalensis* and *Pomatoschistus microps*. Aquat. Toxicol. 102 (3–4):216–227. https://doi.org/10.1016/j.aquatox.2011.01.018.

Gbem, T.T., Balogun, J.K., Lawal, F.A., Annune, P.A., 2001. Trace metal accumulation in *Clarias gariepinus* (Teugels) exposed to sublethal levels of tannery effluent. Sci. Total Environ. 271 (1), 1–9.

Gonzalez, P., Dominique, Y., Massabuau, J.C., Boudou, A., Bourdineaud, J.P., 2005. Comparative effects of dietary methylmercury on gene expression in liver, skeletal muscle, and brain of the zebrafish (*Danio rerio*). Environ. Sci. Technol. 39 (October 2015): 3972–3980. https://doi.org/10.1021/es0483490.

Gray, J.E., Theodorakos, P.M., Bailey, E.A., Turner, R.R., 2000. Distribution, speciation, and transport of mercury in stream-sediment, stream-water, and fish collected near abandoned mercury mines in southwestern Alaska, USA. Sci. Total Environ. 260 (1), 21–33.

Guzzi, G., La Porta, C.A.M., 2008. Molecular mechanisms triggered by mercury. Toxicology 244 (1):1–12. https://doi.org/10.1016/j.tox.2007.11.002.

Habig, W.H., Pabst, M.J., Jakoby, W.B., 1974. Glutathione S-transferases the first enzymatic step in mercapturic acid formation. J. Biol. Chem. 249 (22), 7130–7139.

Haines, T.A., Komov, V., Jagoe, C.H., 1992. Lake acidity and mercury content of fish in Darwin National Reserve, Russia. Environ. Pollut. 78 (1), 107–112.

Han, Z.-X., Wu, D.-D., Wu, J., Lv, C.-X., Liu, Y.-R., 2014. Effects of ocean acidification on toxicity of heavy metals in the bivalve *Mytilus edulis* L. Synth. React. Inorg., Met.-Org., Nano-Met. Chem. 44 (1):133–139. https://doi.org/10.1080/15533174.2013.770753.

Harley, C.D.G., Hughes, A.R., Kristin, M., Miner, B.G., Sorte, C.J.B., Carol, S., 2006. The impacts of climate change in coastal marine systems. Ecol. Lett. 9, 228–241.

Harris, R.C., Bodaly, R.A.D., 1998. Temperature, growth and dietary effects on fish mercury dynamics in two Ontario lakes. Biogeochemistry 40 (2–3), 175–187.

Harvey, B.P., Gwynn-Jones, D., Moore, P.J., 2013. Meta-analysis reveals complex marine biological responses to the interactive effects of ocean acidification and warming. Ecol. Evol. 3 (4):1016–1030. https://doi.org/10.1002/ece3.516.

Heuer, R.M., Grosell, M., 2014. Physiological impacts of elevated carbon dioxide and ocean acidification on fish. Am. J. Physiol. Regul. Integr. Comp. Physiol. 307 (9): R1061–R1084. https://doi.org/10.1152/ajpregu.00064.2014.

IPCC, 2014. Climate change 2014: impacts, adaptation, and vulnerability. Part A: global and sectoral aspects. Contribution of Working Group II to the Fifth Assessment Report of the Intergovernmental Panel on Climate Change. Cambridge University Press, Cambridge, United Kingdom and New York, NY, USA.

Iwama, G.K., Thomas, P.T., Forsyth, R.B., Vijayan, M.M., 1998. Heat shock protein expression in fish. Rev. Fish Biol. Fish. 8 (October):35–36. https://doi.org/10.1023/A.

Jezierska, B., Witeska, M., 2006. The metal uptake and accumulation in fish living in polluted waters. Soil and Water Pollution Monitoring, Protection and Remediation. Springer, pp. 107–114.
Johansson, L.H., Borg, L.A.H., 1988. A spectrophotometric method for determination of catalase activity in small tissue samples. Anal. Biochem. 174 (1), 331–336.
Korbas, M., MacDonald, T.C., Pickering, I.J., George, G.N., Krone, P.H., 2012. Chemical form matters: differential accumulation of mercury following inorganic and organic mercury exposures in zebrafish larvae. ACS Chem. Biol. 7 (2), 411–420.
Kroeker, K.J., Kordas, R.L., Crim, R.N., Singh, G.G., 2010. Meta-analysis reveals negative yet variable effects of ocean acidification on marine organisms. Ecol. Lett. 13 (11): 1419–1434. https://doi.org/10.1111/j.1461-0248.2010.01518.x.
Kroemer, G., Jäättelä, M., 2005. Lysosomes and autophagy in cell death control. Nat. Rev. Cancer 5 (11):886–897. https://doi.org/10.1038/nrc1738.
Lannig, G., Flores, J.F., Sokolova, I.M., 2006. Temperature-dependent stress response in oysters, *Crassostrea virginica*: pollution reduces temperature tolerance in oysters. Aquat. Toxicol. 79 (3):278–287. https://doi.org/10.1016/j.aquatox.2006.06.017.
Lapointe, D., Pierron, F., Couture, P., 2011. Individual and combined effects of heat stress and aqueous or dietary copper exposure in fathead minnows (*Pimephales promelas*). Aquat. Toxicol. 104 (1), 80–85.
Lesser, M.P., 2006. Oxidative stress in marine environments: biochemistry and physiological ecology. Annu. Rev. Physiol. 68 (3):253–278. https://doi.org/10.1146/annurev.physiol.68.040104.110001.
Lewis, E., Wallace, D.W.R., 1998. Program Developed for the CO2 System Calculations. Brookhaven National Lab., Dept. of Applied Science, Upton, NY (United States) Oak Ridge National Lab., Carbon Dioxide Information Analysis Center, TN (United States), Report ORNL/CDIAC-105.
Li, Y., Wang, W.-X., Wang, M., 2017. Alleviation of mercury toxicity to a marine copepod under multigenerational exposure by ocean acidification. Sci. Rep. 7 (1):324. https://doi.org/10.1038/s41598-017-00423-1.
MacLeod, J.C., Pessah, E., 1973. Temperature effects on mercury accumulation, toxicity, and metabolic rate in rainbow trout (Salmo gairdneri). J. Fish. Board Canada 30 (4), 485–492.
Maulvault, A.L., Custodio, A., Anacleto, P., Repolho, T., Pousao, P., Nunes, M.L., Diniz, M., Rosa, R., Marques, A., 2016. Bioaccumulation and elimination of mercury in juvenile seabass (*Dicentrarchus labrax*) in a warmer environment. Environ. Res. 149:77–85. https://doi.org/10.1016/j.envres.2016.04.035.
Maulvault, A.L., Barbosa, V., Alves, R., Custódio, A., Anacleto, P., Repolho, T., Pousão Ferreira, P., Rosa, R., Marques, A., Diniz, M., 2017. Ecophysiological responses of juvenile seabass (*Dicentrarchus labrax*) exposed to increased temperature and dietary methylmercury. Sci. Total Environ. 586:551–558. https://doi.org/10.1016/j.scitotenv.2017.02.016.
Mehrbach, C., Culberson, C.H., Hawley, J.E., Pytkowicx, R.M., 1973. Measurement of the apparent dissociation constantes of carbonic acid in seawater at atmospheric pressure. Limnol. Oceanogr. 18, 897–907.
Melzner, F., Thomsen, J., Koeve, W., Oschlies, A., Gutowska, M.A., Bange, H.W., Hansen, H.P., Kortzinger, A., 2013. Future ocean acidification will be amplified by hypoxia in coastal habitats. Mar. Biol. 160 (8):1875–1888. https://doi.org/10.1007/s00227-012-1954-1.
Michaelidis, B., Spring, A., Pörtner, H.O., 2007. Effects of long-term acclimation to environmental hypercapnia on extracellular acid-base status and metabolic capacity in Mediterranean fish *Sparus aurata*. Mar. Biol. 150 (6):1417–1429. https://doi.org/10.1007/s00227-006-0436-8.
Mieiro, C.L., Ahmad, I., Pereira, M.E., Duarte, A.C., Pacheco, M., 2010. Antioxidant system breakdown in brain of feral golden grey mullet (*Liza aurata*) as an effect of mercury exposure. Ecotoxicology 19 (6), 1034–1045.
Monfort, M.C., 2010. Present Market Situation and Prospects of Meagre (*Argyrosomus regius*), as an Emerging Species in Mediterranean Aquaculture. FAO.
Njemini, R., Demanet, C., Mets, T., 2005. Comparison of two ELISAs for the determination of Hsp70 in serum. J. Immunol. Methods 306 (1), 176–182.
Noyes, P.D., McElwee, M.K., Miller, H.D., Clark, B.W., Van Tiem, L.A., Walcott, K.C., Erwin, K.N., Levin, E.D., 2009. The toxicology of climate change: environmental contaminants in a warming world. Environ. Int. 35 (6), 971–986.
Nunes, M., Coelho, J.P., Cardoso, P.G., Pereira, M.E., Duarte, A.C., Pardal, M.A., 2008. The macrobenthic community along a mercury contamination in a temperate estuarine system (Ria de Aveiro, Portugal). Sci. Total Environ. 405 (1–3):186–194. https://doi.org/10.1016/j.scitotenv.2008.07.009.
Pimentel, M.S., Faleiro, F., Diniz, M., Machado, J., Pousão-Ferreira, P., Peck, M.A., Pörtner, H.O., Rosa, R., 2015. Oxidative stress and digestive enzyme activity of flatfish larvae in a changing ocean. PLoS One 10 (7), e0134082. https://doi.org/10.1371/journal.pone.0134082.
Ponce, R.A., Bloom, N.S., 1991. Effect of pH on the bioaccumulation of low level, dissolved methylmercury by rainbow trout (*Oncorhynchus mykiss*). Water Air Soil Pollut. 56 (1), 631–640.
Portner, H.O., 2002. Climate variations and the physiological basis of temperature dependent biogeography: systemic to molecular hierarchy of thermal tolerance in animals. Comp. Biochem. Physiol. A Mol. Integr. Physiol. 132 (4):739–761. https://doi.org/10.1016/S1095-6433(02)00045-4.
Quinn, G.P., Keough, M.J., 2002. Experimental Design and Data Analysis for Biologists. Cambridge University Press.
R Development Core Team, 2016. R: A Language and Environment for Statistical Computing. (online) Available from:. www.R-project.org.
Rajeshkumar, S., Munuswamy, N., 2011. Impact of metals on histopathology and expression of HSP 70 in different tissues of Milk fish (*Chanos chanos*) of Kaattuppalli Island, South East Coast, India. Chemosphere 83 (4), 415–421.
Repolho, T., Baptista, M., Pimentel, M.S., Dionisio, G., Trubenbach, K., Lopes, V.M., Lopes, A.R., Calado, R., Diniz, M., Rosa, R., 2014. Developmental and physiological challenges of octopus (*Octopus vulgaris*) early life stages under ocean warming. J. Comp. Physiol. B Biochem. Syst. Environ. Physiol. 184 (1):55–64. https://doi.org/10.1007/s00360-013-0783-y.
Rosa, R., Seibel, B.A., 2008. Synergistic effects of climate-related variables suggest future physiological impairment in a top oceanic predator. Proc. Natl. Acad. Sci. 105 (52): 20776–20780. https://doi.org/10.1073/pnas.0806886105.
Rosa, R., Pimentel, M.S., Boavida-Portugal, J., Teixeira, T., Trübenbach, K., Diniz, M., 2012. Ocean warming enhances malformations, premature hatching, metabolic suppression and oxidative stress in the early life stages of a keystone squid. PLoS One 7 (6), e38282.
Rosa, R., Trübenbach, K., Repolho, T., Pimentel, M., Faleiro, F., Boavida-Portugal, J., Baptista, M., Lopes, V.M., Dionísio, G., Leal, M.C., Calado, R., Pörtner, H.O., 2013. Lower hypoxia thresholds of cuttlefish early life stages living in a warm acidified ocean. Proc. Biol. Sci. 280 (1768), 20131695. https://doi.org/10.1098/rspb.2013.1695.
Rosa, R., Trübenbach, K., Pimentel, M.S., Boavida-Portugal, J., Faleiro, F., Baptista, M., Dionísio, G., Calado, R., Pörtner, H.O., Repolho, T., 2014a. Differential impacts of ocean acidification and warming on winter and summer progeny of a coastal squid (*Loligo vulgaris*). J. Exp. Biol. 217:518–525. https://doi.org/10.1242/jeb.096081.
Rosa, R., Lopes, A.R., Pimentel, M., Faleiro, F., Baptista, M., Trubenbach, K., Narciso, L., Dionísio, G., Pegado, M.R., Repolho, T., Calado, R., Diniz, M., 2014b. Ocean cleaning stations under a changing climate: biological responses of tropical and temperate fish-cleaner shrimp to global warming. Glob. Chang. Biol. 20 (10):3068–3079. https://doi.org/10.1111/gcb.12621.
Rosa, R., Paula, J.R., Sampaio, E., Pimentel, M., Lopes, A.R., Baptista, M., Guerreiro, M., Santos, C., Campos, D., Almeida-Val, V.M.F., Calado, R., Diniz, M., Repolho, T., 2016. Neuro-oxidative damage and aerobic potential loss of sharks under elevated CO_2 and warming. Mar. Biol. 163 (5). https://doi.org/10.1007/s00227-016-2898-7.
Sampaio, E., Maulvault, A.L., Lopes, V.M., Paula, J.R., Barbosa, V., Alves, R., Pousão-Ferreira, P., Repolho, T., Marques, A., Rosa, R., 2016. Habitat selection disruption and lateralization impairment of cryptic flatfish in a warm, acid, and contaminated ocean. Mar. Biol. 163 (10):217. https://doi.org/10.1007/s00227-016-2994-8.
Sampaio, E., Rodil, I.F., Vaz-Pinto, F., Fernández, A., Arenas, F., 2017. Interaction strength between different grazers and macroalgae mediated by ocean acidification over warming gradients. Mar. Environ. Res. 125:25–33. https://doi.org/10.1016/j.marenvres.2017.01.001.
Sappal, R., MacDonald, N., Fast, M., Stevens, D., Kibenge, F., Siah, A., Kamunde, C., 2014. Interactions of copper and thermal stress on mitochondrial bioenergetics in rainbow trout, *Oncorhynchus mykiss*. Aquat. Toxicol. 157, 10–20.
Sarazin, G., Michard, G., Prevot, F., 1999. A rapid and accurate spectroscopic method for alkalinity measurements in sea water samples. Water Res. 33 (1):290–294. https://doi.org/10.1016/S0043-1354(98)00168-7.
Scerbo, R., Barghigiani, C., 1998. Organic mercury determination in fish samples using an automatic mercury analyser. Environ. Technol. 19 (3), 339–342.
Schiedek, D., Sundelin, B., Readman, J.W., Macdonald, R.W., 2007. Interactions between climate change and contaminants. Mar. Pollut. Bull. 54:1845–1856. https://doi.org/10.1016/j.marpolbul.2007.09.020.
Sokolova, I., Lannig, G., 2008. Interactive effects of metal pollution and temperature on metabolism in aquatic ectotherms: implications of global climate change. Clim. Res. 37:181–201. https://doi.org/10.3354/cr00764.
Sokolova, I.M., Sukhotin, A.A., Lannig, G., 2011. Stress effects on metabolism and energy budgets in mollusks. Oxidative Stress Aquat. Ecosyst, pp. 261–280.
Sun, Y.I., Oberley, L.W., Li, Y., 1988. A simple method for clinical assay of superoxide dismutase. Clin. Chem. 34 (3), 497–500.
Tiedke, J., Cubuk, C., Burmester, T., 2013. Environmental acidification triggers oxidative stress and enhances globin expression in zebrafish gills. Biochem. Biophys. Res. Commun. 441 (3), 624–629.
Uchiyama, M., Mihara, M., 1978. Determination of malonaldehyde precursor in tissues by thiobarbituric acid test. Anal. Biochem. 86 (1), 271–278.
Vergilio, C.S., Carvalho, C.E.V., Melo, E.J.T., 2012. Accumulation and histopathological effects of mercury chloride after acute exposure in tropical fish *Gymnotus carapo*. J. Chem. Health Risks 2 (4), 1–8.
Vieira, L.R., Gravato, C., Soares, A.M.V.M., Morgado, F., Guilhermino, L., 2009. Acute effects of copper and mercury on the estuarine fish *Pomatoschistus microps*: linking biomarkers to behaviour. Chemosphere 76 (October 2015):1416–1427. https://doi.org/10.1016/j.chemosphere.2009.06.005.
Wagner, A., Boman, J., 2003. Biomonitoring of trace elements in muscle and liver tissue of freshwater fish. Spectrochim. Acta B At. Spectrosc. 58 (12), 2215–2226.
Wang, L., Groves, M.J., Hepburn, M.D., Bowen, D.T., 2000. Glutathione S-transferase enzyme expression in hematopoietic cell lines implies a differential protective role for T1 and A1 isoenzymes in erythroid and for M1 in lymphoid lineages. Haematologica 85 (6), 573–579.
Wang, M., Lee, J.-S., Li, Y., 2017. Global proteome profiling of a marine copepod and the mitigating effect of ocean acidification on mercury toxicity after multigenerational exposure. Environ. Sci. Technol. 51:5820–5831. https://doi.org/10.1021/acs.est.7b01832.
Wiener, J.G., Fitzgerald, W.F., Watras, C.J., Rada, R.G., 1990. Partitioning and bioavailability of mercury in an experimentally acidified Wisconsin lake. Environ. Toxicol. Chem. 9: 909–918. https://doi.org/10.1002/etc.5620090709.
Williams, J.H., Petersen, N.S., Young, P.A., Stansbury, M.A., Farag, A.M., Bergman, H.L., 1996. Accumulation of hsp70 in juvenile and adult rainbow trout gill exposed to metal-contaminated water and/or diet. Environ. Toxicol. Chem. 15 (8), 1324–1328.
Wren, C.D., Scheider, W.A., Wales, D.L., Muncaster, B.W., Gray, I.M., 1991. Relation between mercury concentrations in walleye (*Stizostedion vitreum vitreum*) and northern pike (*Esox lucius*) in Ontario lakes and influence of environmental factors. Can. J. Fish. Aquat. Sci. 48 (1), 132–139.